Numerical Analysis of the Motion and Load Responses of a 400,000 DWT Ore Carrier in Waves

Christiaan Adika Adenya[a, b], Hui-Long Ren[a], Chuan-Dong Qing[a]

[a] College of Shipbuilding Engineering
Harbin Engineering University
Harbin 150001, China.
E-mail: renhuilong@263.net

[b] Department of Marine and Maritime Operations
Jomo Kenyatta University of Agriculture and Technology
Nairobi, Kenya.
E-mail: cadenya@yahoo.com

***Abstract*—The need to benefit from economy of scale has driven the design of larger and larger ships with increasing tonnage. The hull structures of large ships are more flexible and the natural frequencies of the hull girder can even fall within the range of wave encounter frequencies resulting in the resonance phenomenon termed springing. A numerical linear hydroelastic investigation of the wave induced motion and load responses of a 400,000 dead weight tonnage (DWT) ore carrier is carried out in this work using an in-house program: Linear Elastic Compass Wave Loads Calculation System (WALCS-LE). The full load condition at different ship speeds, wave lengths and incident wave headings in regular waves is investigated. Long term predictions are also made. It is imperative to account for springing loads and the probable extreme motions and loads at the design stage of large ships to ensure their endurance and safety at sea.**

Keywords— springing; motion response; wave load; very large ore carrier (VLOC); long-term prediction

I. INTRODUCTION

The need to ensure sufficient energy for a growing world population along with the transportation essential to a globalized economy has fueled increases in ship sizes, to benefit from economy of scale [1], by carrying as much amounts of cargo as possible in one ship trip. The trend of seagoing vessels becoming faster and larger has been accelerated by the rapid increase of global trade [2]. For example, the continuous growth of the Chinese economy demands an increasing supply of ore and energy resources, which has necessitated the design and optimization of very large ore carriers [3]. To reduce weight while at the same time providing the required structural strength, more high-strength steel plates have been used in ship hulls, and this has resulted in reduction of the structural rigidity [3, 4]. Large ships are therefore relatively more flexible and their structural natural frequencies can fall within the range of the wave encounter frequencies in an ordinary sea spectrum [5], which results in springing vibrations. Springing is the continuous hull girder vibrations as a consequence of resonance with waves encounter frequencies [6]. Springing results in high frequency vibration cycles of the hull structure and therefore more attention should be paid to the response of large ships in waves to prevent structural damage and material failure due to fatigue. Precise estimation of the springing-induced hull girder wave loads is critical in guiding the design stage so as to incorporate these loads to prevent hull girder failure due fatigue damage caused by springing vibrations [7]. Knowledge of these loads would also be important for the instruction of the ship's operation during its lifetime and for improving classification rules [5].

In this study, a 400,000 dead weight tonnage (DWT) ore carrier prototype was investigated to evaluate its hydroelastic response in waves. Numerical analyses by the hydroelasticity theory were done based on a linear elastic in-house code: Linear Elastic Compass Wave Loads Calculation System (WALCS-LE). First, the motion response of heave and pitch, and the load response of vertical bending moment amidships as well as shear force at the section 0.25L from the after perpendicular (AP) are sampled and analyzed. Secondly, long term predictions of motion and load response values, based on the summation of short-term probabilities of exceedance of all possible combinations of wave periods, significant wave heights, heading angles and speeds are also made, to inform the ship design and classification rules.

II. LINEAR HYDROELASTICITY THEORY

Linear hydroelasticity is based on beam theory and three dimensional linear potential flow theory. The boundary conditions are assumed linear on both the body and free surface. According to a theory by Rayleigh, any distortion of a beam may be expressed as an aggregate of distortions in its principal modes [8]. Usually, the ship structure is considered as a beam and the structural deflections of a floating slender ship can be expressed by the free undamped 'wet' bending modes of the hull in water [9]. The hydrodynamic force F^h is divided into two parts: F^R which depends on the structural deformations, and F^{DI} which represents the pure excitation [5].

$$F^h = F^R + F^{DI} \tag{1}$$

Using modal superposition, the vector of the wetted surface of deformations $H(x,y,z)$ can be presented as a series of dry natural modes $h_i(x,y,z)$:

$$\begin{aligned} H(x,y,z) &= \sum_{i=1}^{N} h_i(x,y,z) \\ &= \sum_{i=1}^{N} \xi_i \left[h_x^i(x,y,z)\mathbf{i} + h_y^i(x,y,z)\mathbf{j} + h_z^i(x,y,z)\mathbf{k} \right] \end{aligned} \tag{2}$$

This paper is funded by the International Exchange Program of Harbin Engineering University for Innovation-oriented Talents Cultivation

where $h_i(x,y,z)$ denotes the general motion/deformation mode and ξ_i are unknown coefficients.

The total velocity potential φ, is defined by the Laplace differential equation and the following boundary conditions:

$$\begin{aligned} &\Delta\varphi = 0 && \text{within the fluid} \\ &-v\varphi + \frac{\partial \varphi}{\partial z} = 0 && \text{at the free surface, } z = 0 \\ &\frac{\partial \varphi}{\partial n} = -\boldsymbol{i}\omega H n && \text{on the wetted body surface, } S \end{aligned} \tag{3}$$

where $v = \omega^2/g$ is the wave number, ω is wave frequency, n is the wetted surface normal and $\boldsymbol{i}$ is the imaginary unit.

Velocity potential is decomposed into incident wave potential, φ_I, diffraction potential, φ_D, and radiation potential, φ_{Rj}, components:

$$\varphi = \varphi_I + \varphi_D + \boldsymbol{i}\omega \sum_{j=1}^{N} \xi_j \varphi_{Rj} \tag{4}$$

The linearized pressure is given by the Bernoulli's equation:

$$p = \boldsymbol{i}\omega\rho\varphi - \rho g z \tag{5}$$

The hydrodynamic forces are obtained by integrating the pressure over the wetted surface. The excitation and radiation components are determined by considering the pressure term associated with the velocity potential, i.e., $\boldsymbol{i}\omega\rho\varphi$ while the hydrostatic component is determined by considering the hydrostatic term, i.e., $-\rho gz$. The coupled dynamic motion equation in matrix form is given by:

$$\left\{-\omega^2\left([\mathrm{m}]+\left[\mathrm{A}(\omega)\right]\right)+\mathrm{i}\omega\left([\mathrm{d}]+\left[\mathrm{B}(\omega)\right]\right)+\left([\mathrm{k}]+[\mathrm{C}]\right)\right\}\{\xi\}=\{\mathrm{F}\} \tag{6}$$

where ω is encounter frequency, [m] is structural mass, [A(ω)] is added mass, [d] is structural damping, [B(ω)] is hydrodynamic damping, [k] is structural stiffness, [C] is restoring stiffness, {ξ} is modal amplitudes, and {F} is wave excitation force. The solution of (6) gives the modal amplitudes.

III. Prototype Parameters and Model Set-up

A. Hydrodynamic Model

The numerical analysis was performed in the frequency-domain to determine the wave loads experienced by the ore carrier and its motions in regular waves of infinite water depths. The WALC-LE numerical code is based on three-dimensional frequency-domain velocity potential theory and takes into consideration the elastic deformation of the ship hull girder. Modal calculation of the hull girder in wet condition is done by the transfer matrix method. The principal parameters of the prototype ore carrier are tabulated in Tab. 1, where VCG, LCG, and AP denote vertical position of centre of gravity, longitudinal position of centre of gravity, and after-perpendicular, respectively. The full load condition, of ore of density 1.73275 t/m3 with a displacement of 450,851 tons was investigated. The hydrodynamic mesh of the ore carrier is shown in Fig. 1. The mesh has 1752 panels of which 1429 are below the waterline. The hydroelastic model was divided into 20 blocks at 21 cross-sections, the first section being at the stern and the last one at the bow. The cross-sectional area, vertical position of the centroid, shear centre, second moment of area, and mass moment of inertia were determined for each section. For each block, the mass and its centroid were also determined. The mass includes both the cargo and the light weight. The mass distribution for the blocks was checked to ensure that they resulted in the same centre of gravity as that of the whole ship.

B. Simulation Parameters and Setup

Simulations were carried out for infinite water depths, for 12 wave headings starting from 0° to 330° in steps of 30°, and at ship's forward speeds of 0, 5 knots, and 15 knots. The three forward speeds were selected as representative of the ship's motions during its lifetime: zero speed when the ship is still in waves, 5 knots when the ship is sailing in severe waves and 15 knots when the ship is sailing at its design speed. The critical damping coefficient was taken as 0.05. Heave and pitch motion responses, vertical bending moment (VBM) amidships and shear force at 0.25L from AP load responses were selected for investigation in regular waves of frequencies ranging from 0.01 rad/s to 3 rad/s in steps of 0.01 rad/s.

TABLE I. Principal parameters

Item	Value
Length overall (m)	360
Length between perpendiculars (m)	353
Moulded breadth (m)	65
Moulded depth (m)	30.4
Draft at full load (m)	23
Displacement at full load (t)	450,851
Light ship weight (t)	50,500
VCG (from baseline) (m)	14.4
LCG (from AP) (m)	168.41

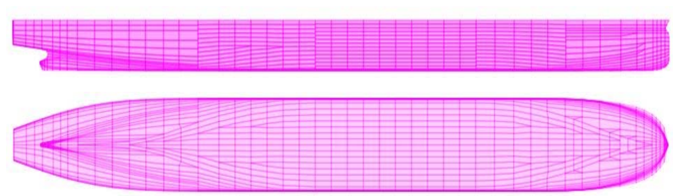

Fig. 1 Hydrodynamic mesh of the ship prototype

IV. Response in Regular Waves

A. Motion Response

Simulation was done to determine the motion response in incident waves of unit amplitude. The response amplitude operators (RAOs) for heave and pitch modes are shown respectively in Fig. 2 (a) and (b) for zero forward speed, Fig. 3 (a) and (b) for 5 knots forward speed, and Fig. 4 (a) and (b) for 15 knots forward speed. From Fig. 2(a), Fig. 3 (a), and Fig. 4 (a), heave motion responses start at 1 m and then reduce to near 0 values as the wave frequency increases from 0 to 1 rad/s. However, for β = 60° wave heading, the heave response first increases to a peak value before reducing steeply to near zero values as the wave frequency increases. A similar trend can also be observed in Fig. 4 (a) for β = 0° heading at 15 knots forward speed. From Fig. 4 (a), a maximum heave response of 1.44 m occurs at a wave frequency of 0.4 rad/s during β = 60° wave heading, and at 15 knots forward ship speed. The heave response for β = 0° and β = 180° headings for wave frequencies 0~0.3 rad/s are the same for zero forward speed as seen in Fig. 2 (a).

The pitch motion responses start at near zero values, rise gradually to a peak values as the wave frequency increases, and then drop to near zero value by about 1 rad/s as shown in Fig. 2 (b), Fig. 3 (b), and Fig. 4 (b). The pitch motion response peaks occur in wave frequencies of range 0.3~0.58 rad/s. The wave heading of β = 120° results in large pitch motion responses during the zero and 5 knot forward speeds as shown in Fig. 2 (b) and Fig. 3 (b) respectively. The maximum pitch motion response was 0.72° at zero forward speed in wave frequency of 0.5 rad/s as seen in Fig. 2 (b). When the forward speed increases from zero to 15 knots, i.e., from Fig. 2 (b) to Fig. 3 (b) to Fig. 4 (b), the maximum pitch motion response values for β = 120° and β = 180° headings reduce while the values for β = 0° and β = 60° headings increase. For example, the maximum pitch response for head waves, i.e., β = 0° heading, increases from 0.46° to 0.61°, whereas for following seas, i.e., β = 180° heading, decreases from 0.47° to 0.35°. In addition, as the forward speed increases, the wave frequency at which the peaks for β = 60° and β = 180° wave headings occur reduce from 0.53 rad/s to 0.47 rad/s and 0.36 rad/s to 0.31 rad/s respectively, while for β = 120° wave heading the peak frequency increased from 0.5 rad/s to 0.59 rad/s. For β = 0° wave heading the peak frequency remains the same at 0.35 rad/s.

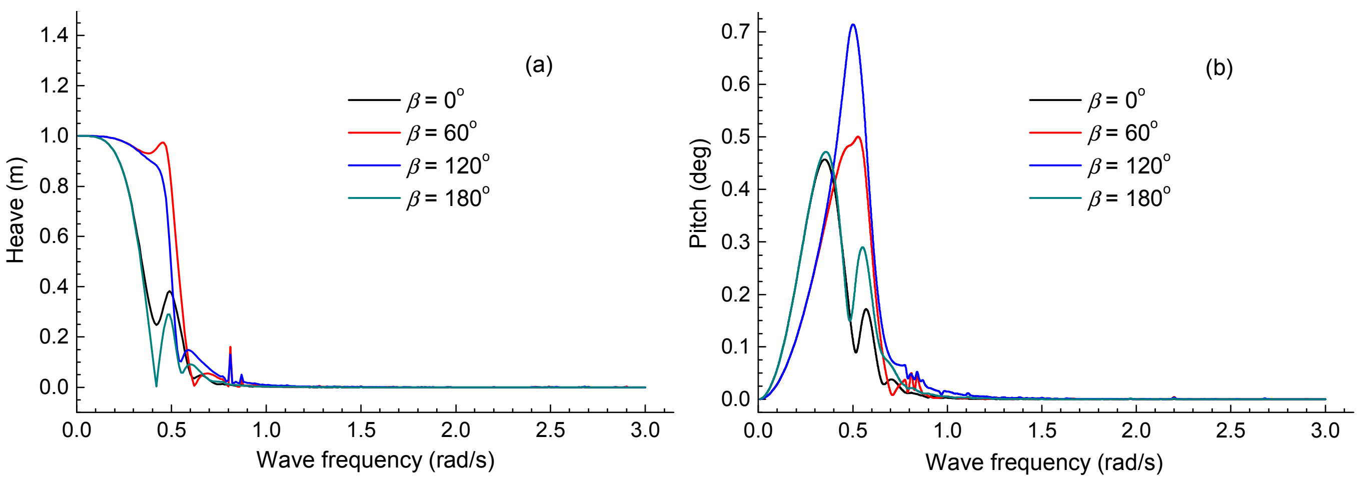

Fig. 2 Motion RAOs for zero forward speed (a) Heave response (b) Pitch response

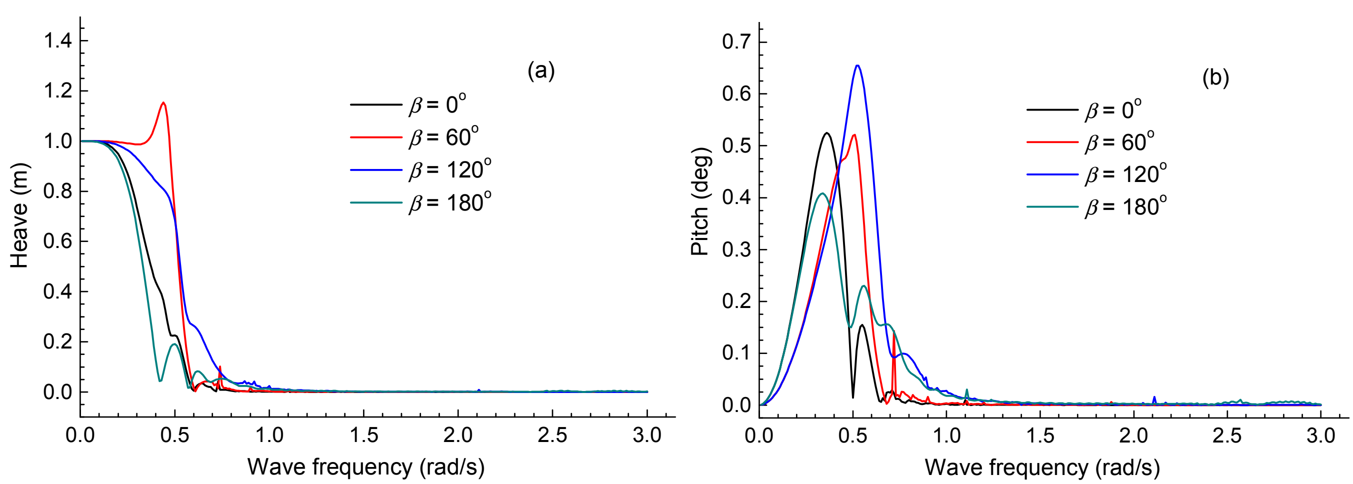

Fig. 3 Motion RAOs for forward speed of 5 knots (a) Heave response (b) Pitch response

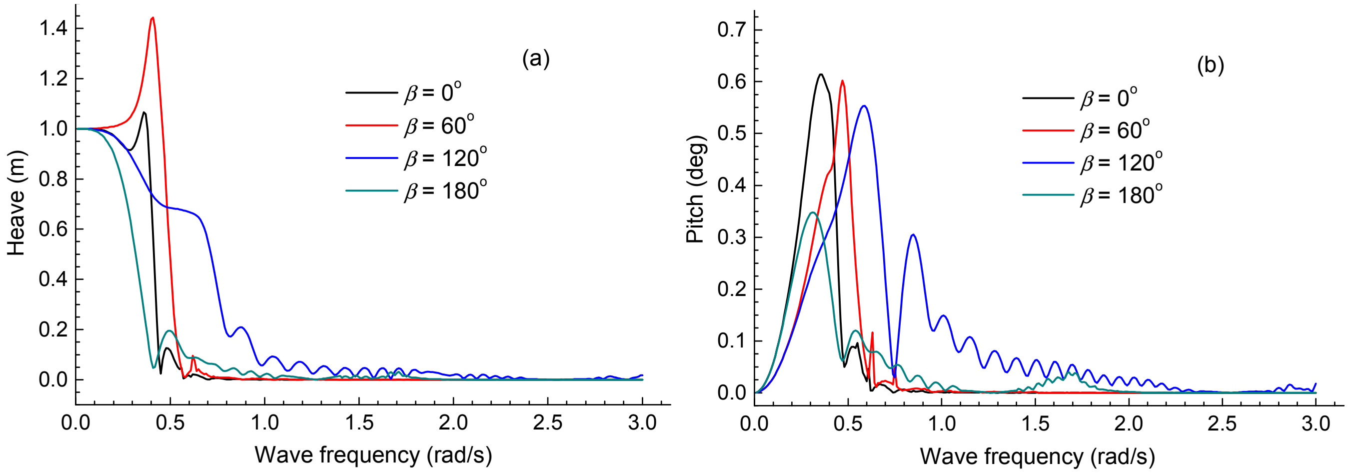

Fig. 4 Motion RAOs for forward speed of 15 knots (a) Heave response (b) Pitch response

B. Load Response

The response amplitude operators (RAOs) were determined for wave-induced loads when the ore carrier when encounters waves of unit amplitude. The RAOs for shear force at the section 0.25L from the after perpendicular (AP) and the vertical bending moment (VBM) amidships are shown respectively in Fig. 5 (a) and (b) for zero forward speed, Fig. 6 (a) and (b) for 5 knots forward speed, and Fig. 7 (a) and (b) for 15 knots forward speed. From the figures, the initial peaks in the low frequency range indicate wave loading response whereas the high peaks in the high frequency range are evidence of the occurrence of the springing response. During springing, the loads are highly magnified due to resonance. At zero forward speed, from Fig. 5 (a) and (b), the major peaks for both the shear force at 0.25L from AP and VBM amidships occur for wave heading of β = 60° at the wave frequencies of 2.2 rad/s and 2.49 rad/s. The values for shear force at 0.25L from AP at these two frequencies are 48.7 MN and 42.8 MN respectively, while for VBM amidships the values are 4.39 GN.m and 4.57 GN.m respectively. The wave heading of β = 120° results in the second highest values of shear force at 0.25L from AP and VBM amidships at the same wave frequencies. There are also other high peaks around the wave frequency of 2.5 rad/s. At 5 knots forward speed, from Fig. 6 (a) and (b), the peak values in the low frequency range remain more or less the same as those for zero forward speed. In the high frequency range, there is however a major peak for both shear force at 0.25L from AP and VBM amidships occurring at a wave frequency of 1.88 rad/s. The peak values are 94.4 MN and 9.24 GNm respectively. The magnitudes are much higher when compared to the zero forward speed case. At 15 knots forward speed, from Fig. 7 (a) and (b), the magnitude of the peaks indicating springing frequencies is lower when compared to zero and 5 knot forward speeds. The peaks for β = 0°, β = 60° and β = 180° wave heading for both shear force and VBM occur at 1.23 rad/s, 1.49 rad/s and 2.5 rad/s. Values of shear force at 0.25L from AP are 36.8 MN, 37.7 MN, and 22.5 MN, while for VBM amidships, the values are 3.78 GNm, 3.74 GNm, and 2.30 GNm. For β = 120°, there is no peak in the high frequency range.

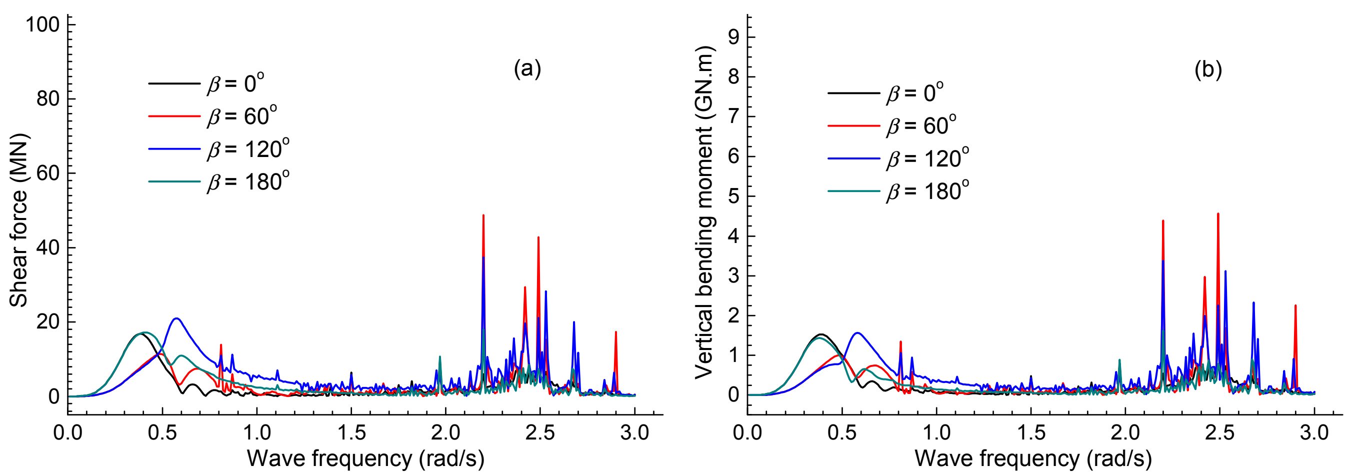

Fig. 5 Load RAOs for zero forward speed (a) Shear force response at 0.25L from AP (b) Vertical bending moment response amidships

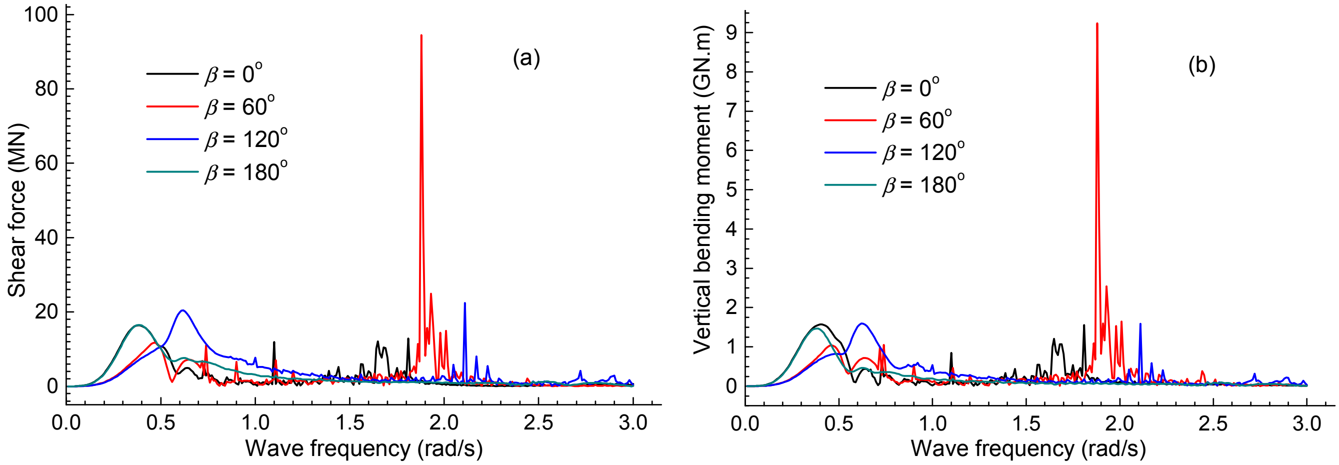

Fig. 6 Load RAOs for forward speed of 5 knots (a) Shear force response at 0.25L from AP (b) Vertical bending moment response amidships

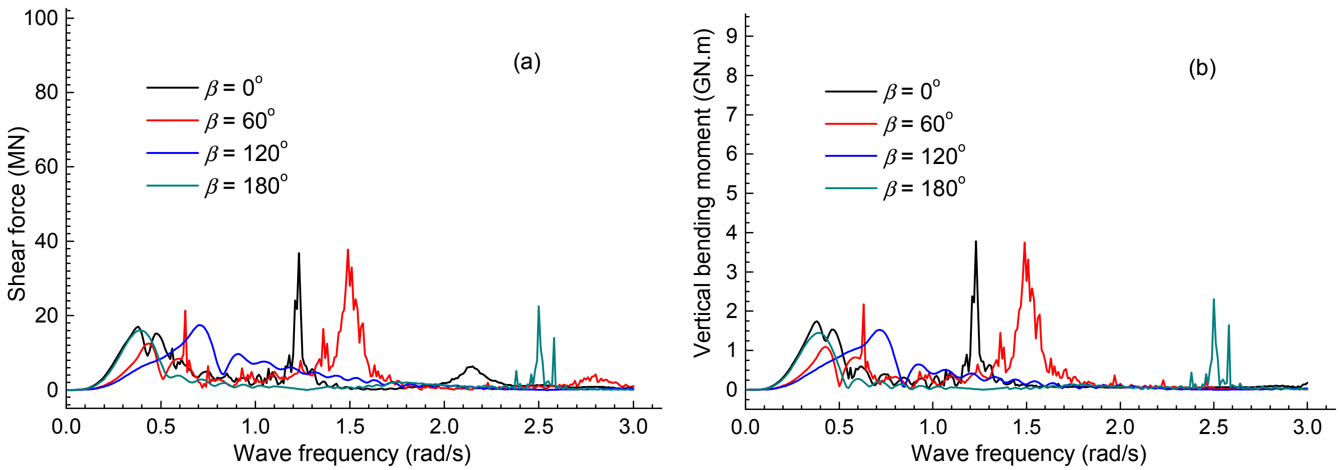

Fig. 7 Load RAOs for forward speed of 15 knots (a) Shear force response at 0.25L from AP (b) Vertical bending moment response amidships

V. Long-term prediction

A. *Long-Term Prediction Theory*

The incident waves and the ship response signals can be regarded as stationary stochastic process by linear theory. The relationship between the incident waves and the ship response in three-dimensional irregular waves can be expressed as [10]:

$$S_w(\omega, H_s, T_z, V, \beta+\theta) = H^2(\omega, V, \beta+\theta) S_\zeta(\omega, H_s, T_z, \theta) \quad (7)$$

where, S_w is ship response spectrum, H is response amplitude operator, S_ζ is incident wave spectrum, ω is wave frequency, H_s is significant wave height, T_z is average zero up-crossing wave period, V is ship speed, β is wave heading, and θ is angle between wave component and main wave direction.

The variance of (7) is obtained by:

$$\begin{aligned} m(H_s, T_z, V, \beta) &= \int_{-\pi/2}^{\pi/2} \int_0^\infty S_w(\omega, H_s, T_z, V, \beta+\theta) d\omega d\theta \\ &= \int_{-\pi/2}^{\pi/2} \int_0^\infty H^2(\omega, V, \beta+\theta) S_\zeta(\omega, H_s, T_z, \theta) d\omega d\theta \end{aligned} \quad (8)$$

The significant amplitude of short-term responses is given by:

$$x_s = 2\sqrt{m(H_s, T_z, V, \beta)} \quad (9)$$

For i^{th} sea state, j^{th} wave heading and k^{th} speed, the probability of exceeding a given value can be obtained by the cumulative Rayleigh distribution function:

$$P_{ijk}(x) = \exp\{-x^2 / E[(H_s, T_z)_i, \beta_j, V_k]\} \quad (10)$$

where, $E[(H_s,T)_i, \beta_j, U_k]$ denotes twice the variance:

$$E[(H_s, T_z)_i, \beta_j, V_k] = 2m(H_s, T_z, V, \beta) \quad (11)$$

Long-term prediction is obtained as a weighted sum of all short-term responses with respect to various sea states, wave headings and ship speeds. The probability of exceedance of ship motions and loads responses at different navigational conditions is given by:

$$P(X \geq x) = \sum_i \sum_j \sum_k p_i(H_s, T_z) p_j(\beta) p_k(V) \exp\left\{ \frac{x^2}{E[(H_s, T_z)_i, \beta_j, V_k]} \right\} \quad (12)$$

where, p_i, p_j, p_k denotes the probability of occurrence of the corresponding condition. The probability of exceedance is the reciprocal of the number of waves encountered by a ship during a given return period. The probability of exceedance of 10^{-8} is usually adopted. This corresponds to a 25 year return period.

B. Results of Long-Term Prediction

Long-term predictions were done for both motion and load responses. Predictions for heave and pitch, VBM amidships and shear force at section 0.25L from AP, for zero, 5 knot and 15 knot forward speeds were considered. The ISSC double parameters spectrum was assumed in the simulation. Predictions were done considering short crested waves with a spreading function of $2cos2\beta/\pi$. The North Atlantic wave scatter diagram was used. The probability of each ship speed was taken as one, whereas the probability of each of the twelve wave headings was equal. Probability of exceedance varied from 10^{-1} to 10^{-8}. Considering the three sailing speeds, Fig. 8 (a)~(d) display the long-term prediction results of the significant amplitude values for the various probabilities of exceedance for heave motion, pitch motion, shear force at 0.25L from AP and VBM amidships, respectively. Considering the average sailing speed of the 400, 000 DWT ore carrier, the predicted extreme values for the probability of exceedance of 10^{-8} are 14 m, 5.90°, 176.5 MN and 15.7 GNm for heave motion, pitch motion, shear force at 0.25L from AP and VBM amidships, respectively.

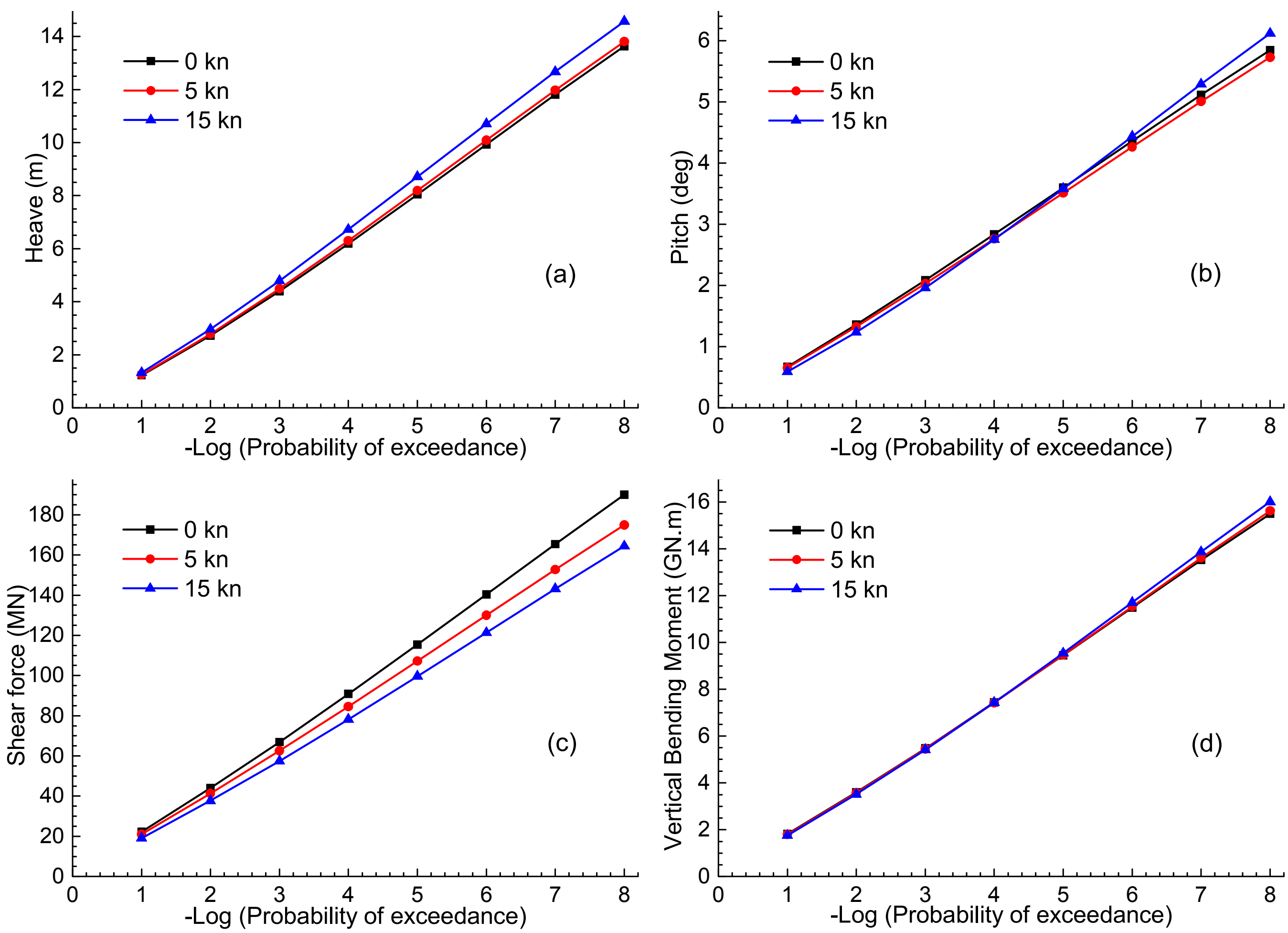

Fig. 8 Results of long-term predictions for (a) Heave (b) Pitch (c) Shear force at 0.25L from AP (d) Vertical bending moment amidships

VI. Conclusion

This paper presented the numerical simulation of motion and load responses as well as the long-term predictions of a 400,000 DWT ore carrier in waves. The WALC-LE, which is based on 3D frequency domain velocity potential theory, and which also takes into account the elastic deformation of the ship hull, is a useful tool in solving the motion and load response problems of very large ships.

The wave headings of 60° and 120° resulted in the largest motion responses for the heave and pitch motions respectively.

The maximum heave responses occurred in wave frequencies of range 0~0.5 rad/s, while for pitch motion they occurred in wave frequencies of range 0.3~0.58 rad/s. The results of the load responses showed the wave frequencies at which springing occurs. Since the springing loads are much larger than the low frequency wave loads, springing must therefore be accounted for at the design stage of large ships. Knowledge of these wave frequencies will also guide the navigation of the ship so as to minimize occurrence of springing.

The long-term prediction results provide valuable insights into the extreme response values that can experienced by the ship in its lifetime. This is important for the ship design and also its navigation.

ACKNOWLEDGMENT

This paper is funded by the International Exchange Program of Harbin Engineering University for Innovation-oriented Talents Cultivation. The authors also greatly appreciate the National Natural Science Foundation of China (Grant No. 51079034) and the National Basic Research Program of China (Grant No. 2011CB013703) for the support provided towards this work.

REFERENCES

[1] ISSC, "Report of technical committee II.2: Dynamic response," in Proceedings of the 18th International Ship and Offshore Structures Congress, Rostock, Germany, 2012, pp. 213-283.

[2] Y. Kim, K.-H. Kim, and Y. Kim, "Analysis of hydroelasticity of floating shiplike structure in time domain using a fully coupled hybrid bem-fem," Journal of Ship Research, vol. 53, pp. 31–47, 2009.

[3] J.-J. Hu, Y.-S. Wu, C. Tian, X.-L. Wang, and F. Zhang, "Hydroelastic analysis and model tests on the structural responses and fatigue behaviours of an ultra-large ore carrier in waves," Proceedings of the Institution of Mechanical Engineers, Part M: Journal of Engineering for the Maritime Environment, vol. 226, pp. 135–155, 2012.

[4] J.-L. Jiao, H.-L. Ren, H. Yang, and D.-L. Mao, "Design of channel-section backbone of segmented model wave load experiment," Journal of Vibration and Shock, vol. 34, pp. 11-15, 2015.

[5] I. Senjanovic, S. Malenica, and S. Tomasevic, "Investigation of ship hydroelasticity," Ocean Engineering, vol. 35, pp. 523-535, 2008.

[6] Y. Lee, et al., "Comparison of springing and whipping responses of model tests with predicted nonlinear hydroelastic analyses," in Proceedings of the 21st International Offshore and Polar Engineering Conference, Maui, Hawaii, USA, 2011, pp. 209-216.

[7] C. D. Jang, J. J. Jung, and A. A. Korobkin, "An approach to estimating the hull girder response of a ship due to springing," Journal of Marine Science and Technology, vol. 12, pp. 95-101, 2007.

[8] R. E. D. Bishop and W. G. Price, Hydroelasticity of ships: Cambridge University Press, 1979.

[9] J. N. Newman, "Wave effects on deformable bodies," Applied Ocean Research, vol. 16, pp. 47-59, 1994.

[10] Y.-S. Dai, J.-W. Shen, and J.-Z. Song, Ship wave loads: National Defense Industry Press, Beijing, 2007.